Yu *et al. Cell Communication and Signaling* (2025) 23:130
https://doi.org/10.1186/s12964-025-02109-y

Cell Communication and Signaling

RESEARCH Open Access

SLC25A35 enhances fatty acid oxidation and mitochondrial biogenesis to promote the carcinogenesis and progression of hepatocellular carcinoma by upregulating PGC-1α

Heng-Chao Yu[1*†], Lu Bai[2†], Liang Jin[1†], Yu-Jia Zhang[3†], Zi-Han Xi[1] and De-Sheng Wang[1*]

Abstract

Mitochondria dysfunction has been closely linked to a wide spectrum of human cancers, whereas the molecular basis has yet to be fully understood. SLC25A35 belongs to the SLC25 family of mitochondrial carrier proteins. However, the role of SLC25A35 in mitochondrial metabolism reprogramming, development and progression in human cancers remains unclear. Here, we found that SLC25A35 markedly reprogramed mitochondrial metabolism, characterized by increased oxygen consumption rate and ATP production and decreased ROS level, via enhancing fatty acid oxidation (FAO). Meanwhile, SLC25A35 also enhanced mitochondrial biogenesis characterized by increased mitochondrial mass and DNA content. Mechanistic studies revealed that SLC25A35 facilitated FAO and mitochondrial biogenesis through upregulating peroxisome proliferator-activated receptor γ coactivator 1α (PGC-1α) via increasing acetyl-CoA-mediated acetylation of PGC-1α. Clinically, SLC25A35 was highly expressed in HCC and correlated with adverse patients' survival. Functionally, SLC25A35 promoted the proliferation and metastasis of HCC cells both in vitro and in vivo, as well as the carcinogenesis in a DEN-induced HCC mice model. Moreover, we found that SLC25A35 upregulation is caused, at least in part, by decreased miR-663a in HCC cells. Together, our results suggest a crucial oncogenic role of SLC25A35 in HCC by reprogramming mitochondrial metabolism and suggest SLC25A35 as a potential therapeutic target for the treatment of HCC.

Keywords SLC25A35, Fatty acid oxidation, Mitochondrial biogenesis, Proliferation, Metastasis, HCC

†Heng-Chao Yu, Lu Bai, Liang Jin and Yu-Jia Zhang contributed equally to this work.

*Correspondence:
Heng-Chao Yu
yuhech1982@163.com
De-Sheng Wang
wangdesh@163.com

[1]Department of Hepatobiliary Surgery, Xijing Hospital, Air Force Medical University, 15 Changle Western Road, Xi'an, Shaanxi 710032, China
[2]Department of Clinical Laboratory, Xijing Hospital, Air Force Medical University, Xian, China
[3]Department of Clinical Medicine, Shaanxi University of Chinese Medicine, Xianyang, China

Introduction

Hepatocellular carcinoma (HCC) is the most common malignant cancer in liver, which represents the fourth leading cause of cancer mortality worldwide [1]. Although great progress has been made in diagnosis and therapy during recent years, the survival of patient with HCC remains unsatisfactory due to the lack of effective therapeutic options for advanced patients with this malignancy [2]. Thus, deepening molecular mechanisms underlying the progression of HCC is urgently needed to uncover new therapeutic biomarkers and strategies.

Metabolism reprogramming has been recognized as a major hallmark of cancer [3]. In addition to enhanced aerobic glycolysis for rapid energy and biosynthetic intermediates supply, fatty acid oxidation (FAO) has also been recognized play a crucial role in malignancy progression of cancer by serving as a major source of adenosine triphosphate (ATP) and NADPH to fulfill energy demand and counteract oxidative stress [4]. Fatty acids are fully oxidized in mitochondria, which serve as the major metabolic hub of the cell [5], through the TCA cycle coupled with oxidative phosphorylation in the electron transport chain (ETC). Although accumulating evidence has revealed the close association between mitochondrial malfunction and cancer [6], the relationship between mitochondrial dysfunction and fatty acid oxidation in the malignant progression of cancer remains largely unknown.

Members of the mitochondrial carrier family (SLC25) play a central role in linking the cytosol and mitochondrial matrix by transporting a variety of compounds across the mitochondria membrane, and their dysfunction have been associated with a large number of diseases and pathologies [7]. SLC25A35 belongs to the SLC25 family of mitochondrial carrier proteins and has been speculated as putative antiporter that exchanges dicarboxylates and sulfur oxoanions across mitochondrial inner [8, 9]. However, the role of SLC25A35 in mitochondrial metabolism reprogramming and disease progression remains unexplored in human cancers. In this work, we find a crucial oncogenic role for SLC25A35 in the carcinogenesis and progression of HCC by reprogramming PGC-1a-mediated mitochondrial fatty acid oxidation and biogenesis via increasing acetyl-CoA-mediated acetylation of PGC1α, suggesting that SLC25A35 might serve as a potential druggable target for the treatment of HCC.

Materials and methods

Tissue samples

A total of 238 pairs of HCC and adjacent non-tumor tissues were obtained from surgical patients at Xijing Hospital of the Air Force Medical University. Of these, 30 pairs were used for qRT-PCR analysis and the remaining 208 pairs were used for Immunohistochemistry (IHC) staining. Informed consents in writing have been obtained from all participates before surgery to use their specimens for research. This study has been approved by the Institutional Ethics Committee of the Xijing Hospital of the Air Force Medical University.

Cell lines

The human HCC cell lines SNU-368, HLE, SNU739, SNU-354, HLF and HUH-7 were purchased from ATCC or the Cell Bank of the Chinese Academy of Sciences in Shanghai. All cell lines were grown in DMEM medium supplemented with 10% FBS at 37 ℃ and tested by short tandem repeat (STR) DNA fingerprinting.

Knockdown or overexpression of interest genes

Small interfering RNAs (siRNAs) or pcDNA3.1 plasmids containing full-length of interest genes were transfected into HCC cells using Lipofectamine 3000 (Thermo Fisher) to achieve knockdown or overexpression. Transfections were conducted according to the manufacturer's instructions. The sequences of siRNAs targeting SLC25A35 were 5'- CGCTTTCTGACACCCATTTTTA C-3' for si-SLC25A35#1 and 5'-GGCATGTACAAGGGT ATAGGTGC – 3' for si-SLC25A35#2.

Quantitative reverse-transcription PCR (qRT-PCR)

Total RNA was extracted using TRIzol reagent (Takara) and reversely transcribed into cDNA using PrimeScript RT Reagent Kit (Takara). The SYBR Green PCR Master Mix (Life Technologies) was used to perform RT-qPCR. β-actin and U6 were used as endogenous controls and the results were calculated by $2^{-\Delta\Delta CT}$ method. The primers utilized in this study were provided in Table S1.

Western blotting analysis

Cells were lysed in RIPA lysis buffer supplemented with protease inhibitor (Roche). Protein concentration was determined by BCA assay. Equal amount of cell lysate was separated by SDS-PAGE and transferred to PVDF membranes. After blocking in 5% milk for 1 h at room temperature, the membranes were incubated with primary antibodies overnight at 4 ℃. After washing, HRP-linked secondary antibody was added and incubated at room temperature for 1.5 h. The blots were visualized by ECL, and β-actin was used as a loading control.

Hematoxylin and eosin (H&E) staining and immunohistochemical (IHC) analysis

Paraffin-embedded tissue sections were firstly deparaffinized and rehydrated. For H&E staining, sections were stained with Mayer's hematoxylin dye for 5 min and then washed with tap water. For IHC analysis, tissue sections were treated for heat-mediated antigen retrieval in citrate buffer, blocked and incubated with specific primary

antibodies listed in Table S2 at 4 °C overnight. After washing, the sections were incubated with HRP-labeled secondary antibody for 1 h and DAB for 5 min at room temperature. The images were obtained using an Olympus microscopy with lightning model.

Cell proliferation and colony formation assays

Cell Counting Kit-8 (CCK-8) assay was used for evaluation of cell proliferation. Cells were seeded in 96-well plates (5000 cells/well) and cultured for indicated time. The CCK8 reagent was added to each well and the absorbance at 450 nm was measured by a microplate reader.

For colony formation assay, HCC cells (500 cells/well) were plated in six-well plate. After culturing for two weeks, colonies were fixed with 4% paraformaldehyde and stained by crystal violet. After washing, the number of colonies was counted.

Cell apoptosis and cycle analysis

Cell apoptosis and cycle distribution were analyzed with a cell apoptosis or cycle kit from US Everbright Inc (#F-6012 and #C-6031) according to their manufacturer's instructions. The results were detected using flow cytometry (Beckman).

Evaluations of oxygen consumption rate (OCR) and contents of ATP and NADPH

The oxygen consumption rate (OCR) was measured with a Seahorse XF96 Extracellular Flux Analyzer as per the manufacturer's instructions. The contents of ATP and NADPH were measured with two commercial kits purchased from Abcam (#ab83355 and #ab65349) following their manufacturer's instructions. The results were measured by a plate reader.

Detections of mitochondrial mass, membrane potential and ROS content

MitoTracker green fluorescent dye purchased from Molecular Probes (#M7514) was used to determine mitochondrial mass according to the manufacturer's instruction. For evaluation of mitochondrial membrane potential, a JC-1 dye purchased from Beyotime Biotechnology (#C2006) was used following the manufacturer's instruction. The content of reactive oxygen species (ROS) was detected by a fluorescent probe DCFH-DA (Beyotime Biotechnology, #S0033) as per the manufacturer's instruction.

Fatty acid oxidation (FAO)

FAO was measured with ^{3}H-labeled oleic acid (Amersham Pharmacia Biotech, Italy) as a tracer. Briefly, cells were seeded to 24-well plate and cultured to about 80% confluence. Fresh culture medium containing ^{3}H-labeled oleic acid (1 μCi) was added to each well and incubated overnight. A L6500 scintillation counter was used to detect the production of $^{3}H_2O$ in each cell sample.

Wound healing assay

HCC cells were seeded in a 6-well plate. When grown to 70–80% confluence, a scratch was made with a 100 μl pipette tip. Wounds were photographed at 0 h and 24 h after scratching. Wound closure (%) was measured using Image J software.

Transwell migration and invasion assays

Cell migration and invasion abilities were evaluated using Transwell chambers without or with matrigel (Corning). Briefly, a total of 5×10^4 cells were seeded in the upper chamber in serum-free medium. Medium with 10% FBS was added to the bottom of the well. After culturing for 24–48 h, migrated or invaded cells were stained with crystal and their numbers were counted under a light microscope.

In vivo tumor xenograft and metastatic animal model

Male BALB/c nude mice (4- to 6-week-old) were maintained in a specific-pathogen-free (SPF) facility under 12-hour light-dark cycles. The study was approved by the animal ethics committee of Xijing Hospital of the Air Force Medical University.

For construction of in vivo tumor xenograft, HCC cells (1×10^7) with indicated treatment were subcutaneously injected into the right flanks of the nude mice. Tumor was monitored and their volumes were measured every 7 days. Animals were finally anesthetized and the tumors were excised for further studies.

For in vivo metastatic nude mice model, 5×10^6 HCC cells with indicated treatment were injected into male BALB/c nude mice through their tail veins. Five weeks post cells injection, animals were anesthetized and their lungs were excised for H&E staining.

Generation of DEN-induced HCC mice model

The 2-week-old male mice were given adeno-associated virus (AAV)-control or AAV-SLC25A35 (1×10^{11} viral genomes in 100 μl saline) by intravenous injection. One week after AAV injection, the mice were intraperitoneal (i.p.) injected with 25 mg/kg DEN. Then the mice were fed normally until the end of the study at 28 weeks post DEN injection and sacrificed using CO_2 chamber. The body weight and liver weight were determined and visible tumors (> 1 mm) were counted.

Measurement of serum ALT and AST

To determine the activities of serum ALT and AST, an Alanine Aminotransferase Assay Kit (C009-2-1) and Aspartate Aminotransferase Assay Kit (#C010-2-1)

purchased from Nanjing Jiancheng Bioengineering Institute were used according to their manufacturer's instructions.

Statistical analysis

SPSS 17.0 software was used for statistical analyses. Results are represented as mean ± SD from at least 3 repeats. Difference between two or more than two groups was determined by Student's t test or one/two-way ANOVA. Patient survival was analyzed by the Kaplan-Meier method and log-rank test. $P < 0.05$ was accepted for statistically significant.

Results

SLC25A35 promotes mitochondrial oxidative respiration and ATP production accompanied by decreased oxidative stress

To elucidate the role of SLC25A35 in mitochondrial metabolism in HCC cells, we knocked-down SLC25A35 expression with two distinct siRNAs in SNU-739 and SNU-354 cells expressing high SLC25A35, and overexpressed SLC25A35 in SNU-368 and HLE cells expressing low SLC25A3, among HCC cell lines tested in Fig S1A and S1B. Successful knockdown and overexpression of SLC25A35 were validated by qRT-PCR and Western blotting analysis (Fig S1C and S1D). Evaluations of oxygen consumption rate (OCR) and extracellular acidification rate (ECAR) using the Seahorse XF96 analyzer revealed markedly decreased or increased OCR when SLC25A35 was silenced or overexpressed in HCC cells (Fig. 1A), while ECAR was not changed significantly (Fig S1E), suggesting that SLC25A35 promotes mitochondrial metabolism with no significant effect on aerobic glycolysis, which is the well-recognized characteristic of cancer cell metabolism also known as the Warburg effect. In agreement with this, significant decreased mitochondrial membrane potential (Fig S1F), activities of mitochondrial respiratory chain complexes I-IV (Fig S1G), contents of ATP (Fig. 1B) and metabolic intermediates in the TCA cycle (Fig. 1C), while increased ROS levels were observed in SLC25A35-knockdown HCC cells (Fig. 1D), which is contrary to our original thoughts that enhanced mitochondrial metabolism would produce more ROS. By contrast, the opposite effects were observed in SLC25A35-overexpressed HCC cells.

To determine the mechanism underling enhanced mitochondrial metabolism by SLC25A35 in HCC cells, the effects of SLC25A35 knockdown or overexpression on mitochondrial morphology was analyzed by transmission electron microscopy (TEM). The results showed that SLC25A35 knockdown or overexpression had no significant effects on mitochondrial length and length-to-width ratio (Fig. 1E), indicating that SLC25A35 promotes mitochondrial metabolism may not through changes in mitochondrial dynamics. In line with this, the expression levels of crucial factors involved in mitochondrial dynamics, including mitochondrial fission factors DRP1, FIS1 and MFF, and mitochondrial fusion factors MFN1, MFN2 and OPA1, were not altered significantly following knockdown or overexpression of SLC25A35 in HCC cells (Fig S1H). When measuring the biogenesis of mitochondrial, we discovered a significant decrease in both the content of mitochondria and mitochondrial DNA (mtDNA) measured by MitoTracker Green staining and qRT-PCR assays when SLC25A35 was knockded-down, whereas the opposite effects were observed when SLC25A35 overexpressed (Fig. 1F and G).

Together, these results suggest that SLC25A35 promotes mitochondrial energy metabolism accompanied by decreased oxidative stress.

Enhanced mitochondrial metabolism by SLC25A35 was principally fueled by fatty acid oxidation

Glucose, fatty acid and amino acid are the three main substrates for mitochondrial metabolism. To clarify the energy source of enhanced mitochondrial metabolism by SLC25A35, the three major metabolic pathways, including glycolysis, fatty acid oxidation (FAO), and glutaminolysis were suppressed by treatment with specific inhibitors. Evaluation of mitochondrial energy metabolism by detecting ATP production indicated that blockage of either glycolysis or glutaminolysis had no significant effect on increased ATP production caused by SLC25A35 overexpression, while inhibition of FAO greatly attenuated the elevation of ATP production induced by SLC25A35 overexpression (Fig. 2A). In line with this, inhibition of FAO greatly attenuated the increase of OCR caused by SLC25A35 overexpression (Fig. 2B), implying that SLC25A35 enhances mitochondrial metabolism mainly by activating fatty acid oxidation. To test this prediction, the effect of SLC25A35 on FAO was evaluated using ^{3}H-labeled oleic acid. We found a significant increase in the rate of FAO upon SLC25A35 overexpression in HCC cells, while a significant decrease of FAO upon SLC25A35 silencing in HCC cells (Fig. 2C). In agreement with this, obviously increased lipid accumulation (Fig. 2D) and triglyceride content (Fig. 2E) were observed in SLC25A35 silencing HCC cells as compared with control, while the opposite were seen in SLC25A35 overexpression HCC cells. Besides energy production, FAO also serves as an important source of NADPH, which plays an important role in the maintenance of redox homeostasis by quenching ROS [4]. Given that SLC25A35 reduces ROS level in HCC cells, we hypothesized that SLC25A35 may reduce ROS level by increasing FAO-mediated NAPDH production. The results showed that NADPH/NADP^{+} ratio were significantly decreased upon SLC25A35 silencing, while increased

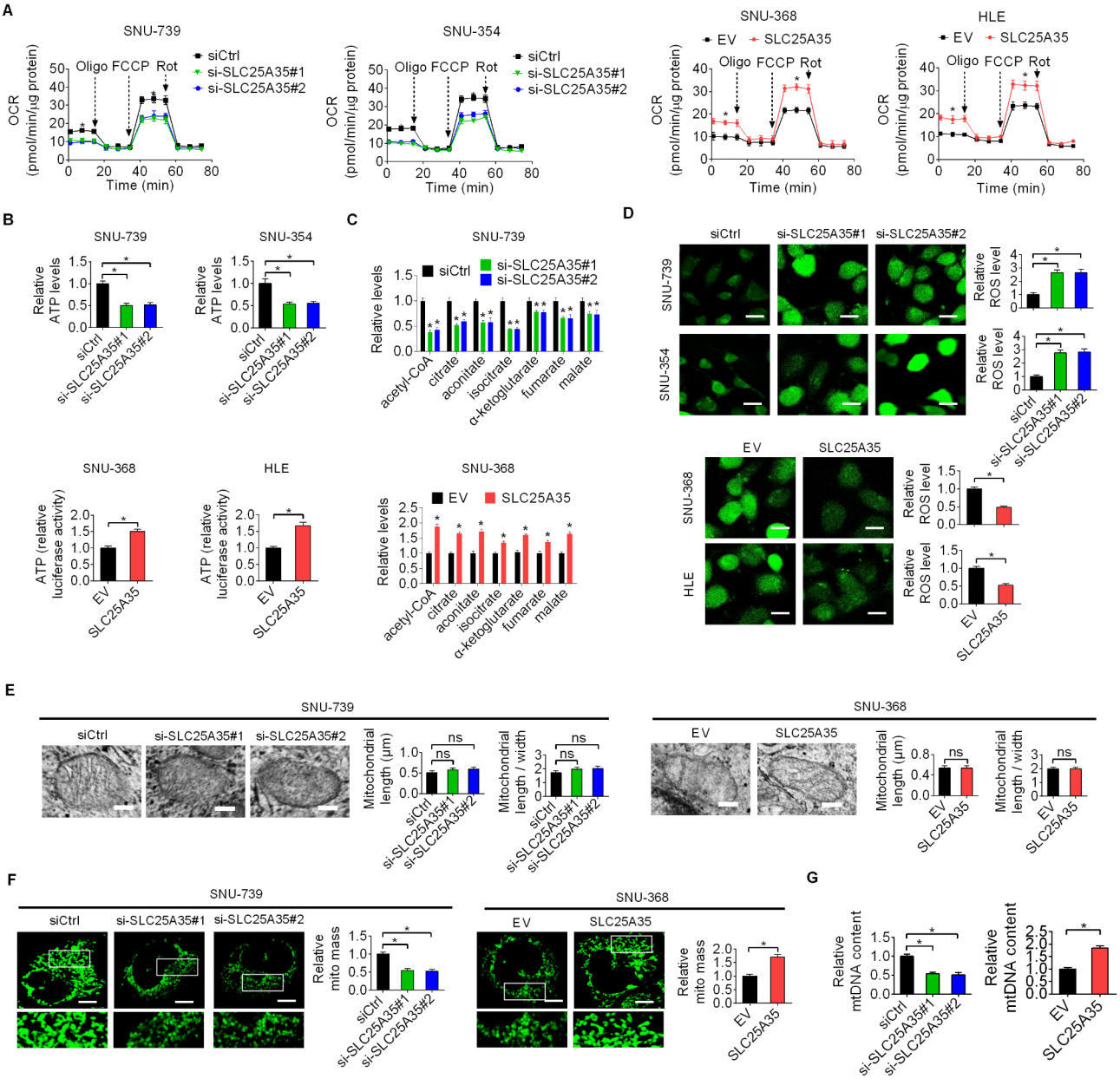

Fig. 1 SLC25A35 promotes metabolism oxidative respiration and ATP production accompanied by decreased oxidative stress. (**A**) Detection of oxygen consumption rate (OCR) using the Seahorse XF96 analyzer in SLC25A35 silenced or overexpressed HCC cells. (Olig, Oligomycin; Rot, Rotenone). (**B-D**) The levels of ATP (**B**), metabolic intermediates in the TCA cycle (**C**) and ROS (**D**) were measured in SLC25A35 silenced or overexpressed HCC cells (D, Scale bars = 20 μm). (**E**) Electron microscopy was used for evaluation of changes in mitochondrial morphology. Representative electron microscopy images of mitochondria are shown in the left panel. Alterations in mitochondrial dynamics was evaluated by mitochondrial length (middle panel) and length-to-width ratio (right panel) (Scale bars = 0.2 μm). (**F**) MitoTracker Green staining assay was used for evaluations of mitochondrial mass in SLC25A35 silenced or overexpressed HCC cells (Scale bars = 5 μm). (**G**) qRT-PCR assay was used to detect the content of mtDNA in SLC25A35 silenced or overexpressed HCC cells

upon overexpression of SLC25A35 in HCC cells (Fig. 2F). Furthermore, we found that suppression of FAO by Etomoxir treatment significantly attenuated the increase of NADPH/$NADP^+$ ratio and ATP production and restored the decrease of ROS level caused by SLC25A35 overexpression (Fig. 2G and I). These findings suggest that the enhanced mitochondrial metabolism by SLC25A35 was fueled principally by FAO to not only satisfy the energy demands but also prevent oxidative stress in HCC cells.

SLC25A35 upregulates PGC-1α expression via facilitating acetyl-CoA-mediated acetylation of PGC1α

We next investigated the mechanism by which SLC25A35 promotes fatty acid oxidation in HCC cells. Using the

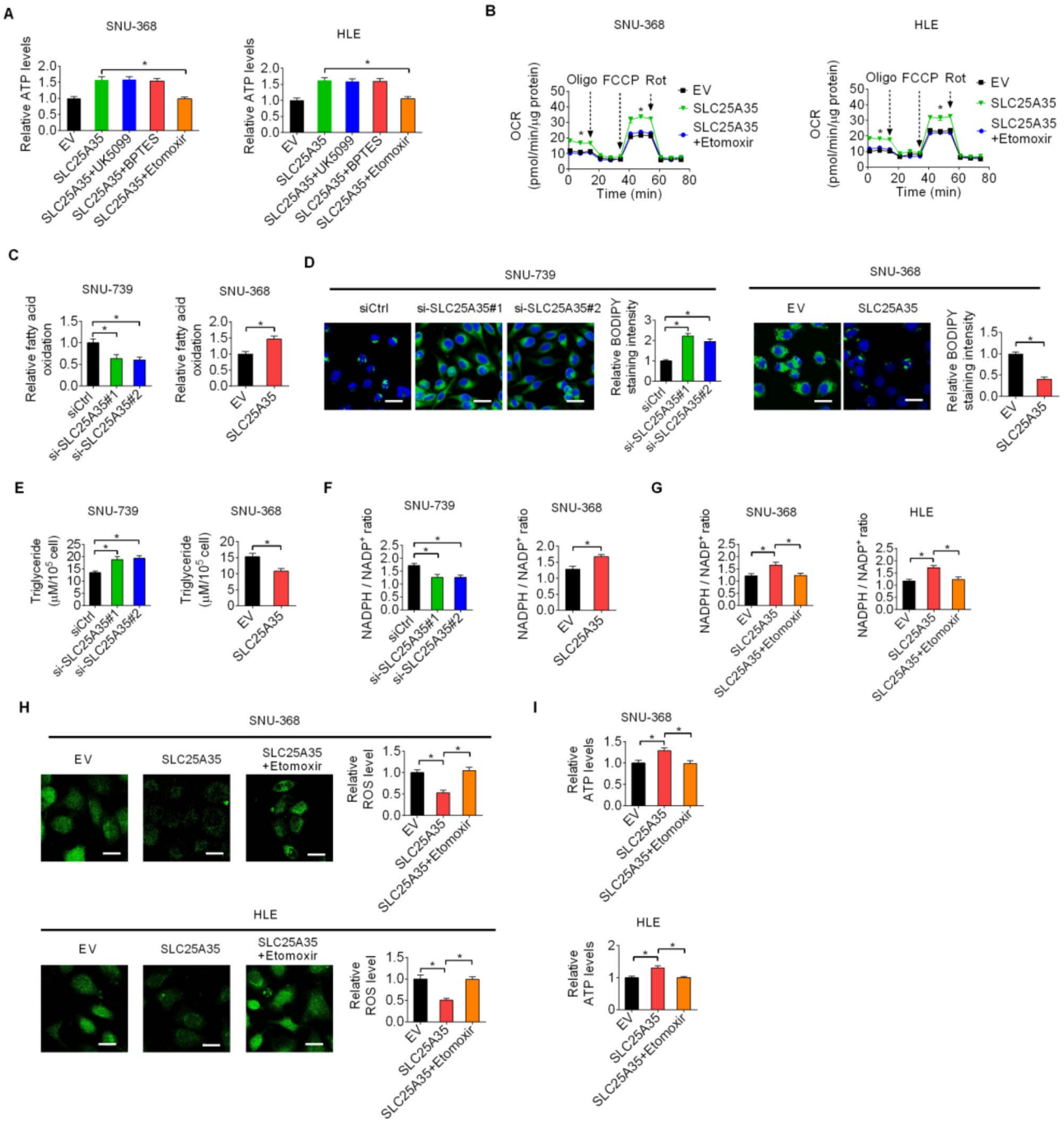

Fig. 2 Enhanced mitochondrial metabolism by SLC25A35 was fueled principally by fatty acid oxidation. (**A**) The effects of UK5009 (20 nM for 72 h), BPTES (100 nM for 72 h) and Etomoxir (100 nM for 72 h) treatments on ATP production was determined in indicated HCC cells. (**B**) Oxygen consumption rate (OCR) was evaluated using the Seahorse XF96 analyzer upon Etomoxir treatment (100 nM for 72 h). (**C**) ^{3}H-labeled oleic acid was used to evaluate fatty acid oxidation in HCC cells upon SLC25A35 silencing or overexpression. (**D** and **E**) Lipid accumulation (**D**) and triglyceride content (**E**) were evaluated in SLC25A35 silenced or overexpressed HCC cells using BODIPY-based immunofluorescence staining assay and a colorimetric assay kit, respectively (D, Scale bars = 20 μm). (**F**) The ratio of NADPH/NADP^{+} was determined in SLC25A35 silenced or overexpressed HCC cells. (**G**-**I**) The ratio of NADPH/NADP^{+} (**G**) and levels of ATP (**H**) and ROS (**I**) were determined in HCC cells treated with Etomoxir (I, Scale bars = 20 μm)

mass spectrometry analysis, we found a total of 8 proteins that were significantly changed (> 2.5 fold change) upon SLC25A35 silencing and overexpressing in HCC cells (Fig. 3A). Among those proteins, peroxisome proliferator-activated receptor gamma coactivator 1-alpha (PGC-1α) has been known as a master transcriptional coactivator that regulates the expressions of multiple enzymes involved in FAO. To confirm the regulation of PGC-1α expression by SLC25A35 in HCC cells, qRT-PCR and western blotting assays were then performed. The results indicated that both total cellular and nuclear expressions of PGC-1α at protein level, but not at mRNA level, was significantly decreased upon SLC25A35 silencing, while increased upon SLC25A35 overexpressing (Fig. 3B and C and Fig S2A), suggesting a post-translational regulatory mechanism of PGC-1α by SLC25A35 in HCC cells. In line with this, a significant positive correlation was found between the expressions of SLC25A35 and PGC-1α in tumor tissues from 208 HCC patients (Fig. 3D). To determine whether the stability of PGC-1α protein was regulated by SLC25A35, protein synthesis in HCC cells was inhibited by CHX. Results showed that SLC25A35 silencing significantly shortened the half-life of PGC-1α, while SLC25A35 overexpression led to extended half-life of PGC-1α (Fig. 3E and Fig S2D). Considering the existence of two major routes, including autophagy-lysosomal pathway and ubiquitin-proteasome pathway, in the degradation of intracellular proteins, we treated SLC25A35-silencing HCC cells with CQ (autophagy-lysosomal inhibitor) and MG132 (proteasome inhibitor), respectively. As shown in Fig. 3F, decreased PGC-1α expression by SLC25A35 silencing was markedly restored by MG132 treatment, but not CQ, suggesting that SLC25A35 silencing downregulates PGC-1α expression by activating the ubiquitin-proteasomal degradation pathway. Expectedly, SLC25A35 silencing obviously enhanced the ubiquitination of PGC-1α, while SLC25A35 overexpression exerted an opposite effect (Fig. 3G).

Next, we explored the precise molecular mechanisms by which SLC25A35 downregulates ubiquitin-proteasomal degradation of PGC-1α in HCC cells. Acetylation has been known to play an important role in the regulation of PGC-1α activity and expression [10]. Given that metabolome analysis in Fig. 1C indicated a positive effect of SLC25A35 on the level of acetyl-CoA, which serves as the donor of acetyl for protein acetylation, we therefore asked whether SLC25A35 regulate PGC-1α expression through acetyl-CoA-mediated protein acetylation. To answer this question, the effects of SLC25A35 on acetyl-CoA level and acetylation of PGC-1α were evaluated. We first used an ELASA assay to confirm the metabolome analysis results in Fig. 1C and found that the total cellular and cytoplasmic levels of acetyl-CoA were positively regulated by SLC25A35 (Fig. 3H). Western blotting assay further showed that the acetylation of PGC-1α was obviously diminished by SLC25A35 knockdown, while enhanced by SLC25A35 overexpression (Fig. 3I), suggesting that SLC25A35 may facilitate the acetylation of PGC-1α by increasing acetyl-CoA level in HCC cells. To further determine whether the acetylation of PGC-1α contribute to its upregulation by SLC25A35 in HCC cells, HCC cells were treated with the inhibitor or agonist of SIRT1, which was reported as a crucial deacetylase of PGC-1α [10]. We found that decreased acetylation and expression of PGC-1α caused by SLC25A35 silencing were significantly rescued by treatment with the SIRT1 inhibitor EX-527. Conversely, increased acetylation and expression of PGC-1α caused by SLC25A35 overexpression were markedly attenuated by treatment with SIRT1 agonist resveratrol (Fig. 3J and K). GCN5 and SIRT1 are responsible for the deacetylation and acetylation of PGC-1α [11]. To provide more insights, we assessed the roles of GCN5 and SIRT1 in SLC25A35-regulated PGC-1α acetylation by examining their interactions with PGC-1α in HCC cells after silencing or overexpressing SLC25A35. The results indicated that SLC25A35 did not significantly affect the interactions between PGC-1α and GCN5 or SIRT1 in HCC cells (Fig S2C). This suggests that SLC25A35 may promote PGC-1α acetylation not by enhancing GCN5-mediated acetylation or reducing SIRT1-mediated deacetylation, but primarily by increasing cytoplasmic acetyl-CoA levels.

Together, these results suggest SLC25A35 upregulates the expression and nuclear translocation of PGC-1α through facilitating cytoplasmic acetyl-CoA-mediated acetylation of PGC1α.

SLC25A35 promotes FAO and mitochondrial biogenesis by upregulating PGC-1α

In light of the well-known role of PGC-1α in FAO and mitochondrial biogenesis [12], we set out to determine whether the SLC25A35 promotes mitochondrial biogenesis and FAO by upregulating PGC-1α. Using ^{3}H-labeled oleic acid, we found that the effect of SLC25A35 silencing on the suppression of FAO was markedly restored by PGC-1α overexpression, while the activation of FAO by SLC25A35 overexpression was abolished by PGC-1α knockdown (Fig. 4A). In line with this, the effect of SLC25A35 silencing or overexpression on lipid accumulation was also markedly rescued by PGC-1α overexpression or knockdown (Fig. 4B and C). In addition, the involvement of PGC-1α in SLC25A35-regulated ATP production and oxidative stress was also explored. The results showed that reduced ATP production and increased oxidative stress caused by SLC25A35 silencing were obviously reversed by PGC-1α overexpression. On the contrary, increased ATP production and decreased oxidative stress caused by SLC25A35 overexpression

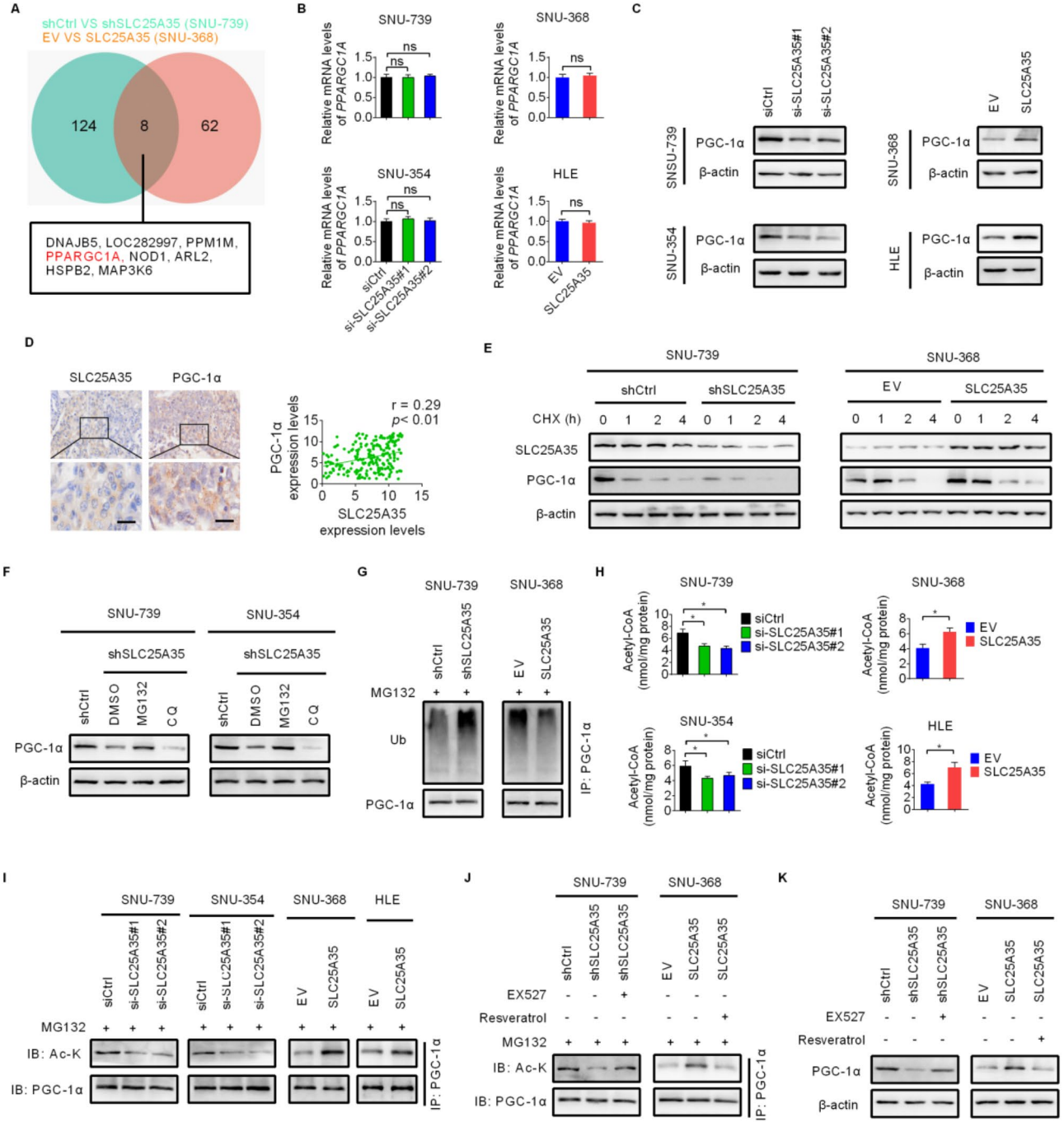

Fig. 3 SLC25A35 upregulates PGC-1α expression via facilitating acetyl-CoA-mediated acetylation of PGC1α. (**A**) Venn diagram for proteins that are significantly changed (> 2.5 fold change) both upon SLC25A35 silencing and overexpressing in HCC cells, as detected by mass spectrometry-based proteomic analysis. (**B** and **C**) qRT-PCR (**B**) and Western blotting (**C**) assays were used to detect PGC-1α expression in indicated HCC cells. (**D**) Immunohistochemistry analysis for the correlation between SLC25A35 and PGC-1α expressions in HCC tumor tissues ($n = 208$) (Scale bars = 20 μm). (**E**) SLC25A35 and PGC-1α expressions were detected by western blotting assay in HCC cells treated with CHX (10 μM). (**F**) PGC-1α expression was detected by western blotting assay in HCC cells treated with MG132 (20 μM) or CQ (20 μM). (**G**) Ubiquitination of PGC-1α was determined western blotting assay in with indicated treatment. (**H**) An ELASA assay was used to evaluate the effect of SLC25A35 on acetyl-CoA level in HCC cells. (**I**) Western blotting assay was used to detect the effect of SLC25A35 on the acetylation of PGC-1α. (**J** and **K**) The acetylation (**J**) and expression (**K**) of PGC-1α were detected by western blotting assay in HCC cells treated with SIRT1 inhibitor EX-527 or agonist resveratrol

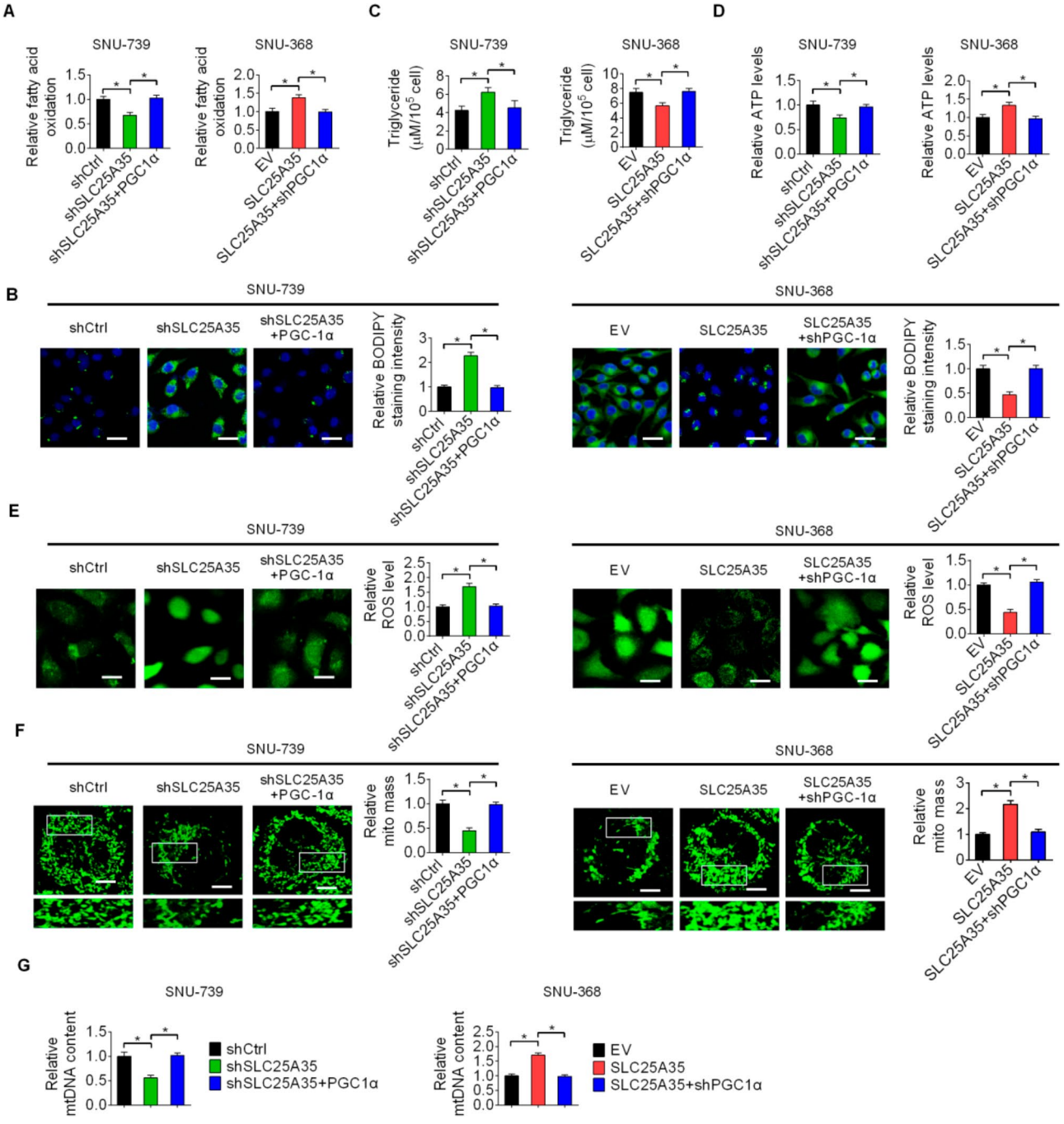

Fig. 4 SLC25A35 promotes FAO and mitochondrial biogenesis by upregulating PGC-1α. (**A**)^{3}H-labeled oleic acid was used to evaluate fatty acid oxidation in HCC cells with indicated treatment. (**B** and **C**) Lipid content was evaluated with a BODIPY-based immunofluorescence staining assay (**B**) and colorimetric assay kit (**C**) in HCC cells with indicated treatment (B, Scale bars = 20 μm). (**D and E**) The levels of ATP (**D**) and ROS (**E**) were measured in HCC cells with indicated treatment. (E, Scale bars = 20 μm). (**F**) MitoTracker Green staining assay was used for evaluation of mitochondrial mass in HCC cells with indicated treatment (Scale bars = 5 μm). (**G**) The content of mtDNA was determined by qRT-PCR assay in HCC cells with indicated treatment

were rescued by PGC-1α knockdown (Fig. 4D and E). Moreover, we also explored whether the effect of SLC25A35 on mitochondrial biogenesis was mediated by PGC-1α. Our results showed that suppression of mitochondrial biogenesis caused by SLC25A35 silencing was reversed by PGC-1α overexpression, while increased mitochondrial biogenesis by SLC25A35 overexpression was impaired by PGC-1α knockdown (Fig. 4F and G).

SLC25A35 is upregulated and correlated with aggressiveness and adverse patients' survival in HCC

The crucial roles of SLC25A35 in mitochondrial biogenesis and FAO prompted us to determine whether SLC25A35 was dysregulated in HCC. Using the UALCAN [13] online database, we found that SLC25A35 was significantly upregulated in HCC tissues as compared with normal liver tissues (Fig. 5A). SLC25A35 upregulation was also confirmed by qRT-PCR analysis in 30 pairs of HCC tumor and adjacent non-tumor tissues (Fig. 5B), as well as by immunohistochemistry (IHC) staining in another 208 pairs of HCC tumor and adjacent non-tumor tissues (Fig. 5C). Analysis of the correlation between SLC25A35 and the clinicopathological features of these patients showed that SLC25A35 expression was positively associated with the size of tumor and the incidence of metastasis (Supplementary Table S3). Additionally, high SLC25A35 expression was associated with a worse overall survival (Fig. 5D) and higher recurrence

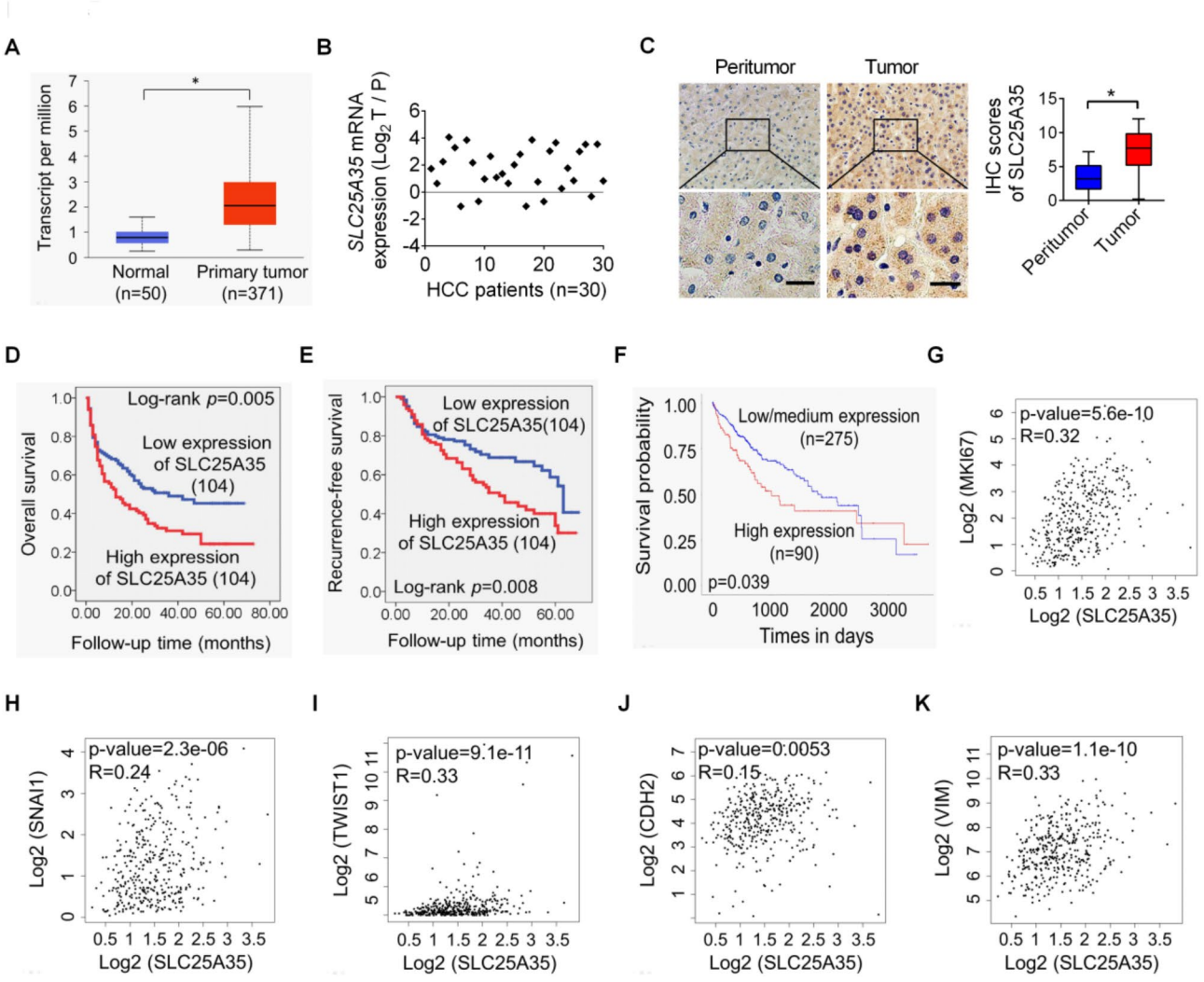

Fig. 5 SLC25A35 is upregulated and correlated with aggressiveness and adverse patients' survival in HCC. (**A**) SLC25A35 expression was analyzed using the online UALCAN database. (**B**) SLC25A35 expression was detected by qRT-PCR analysis in 30 pairs HCC tumor and adjacent non-tumor tissues. (**C**) SLC25A35 expression was evaluated using immunohistochemistry (IHC) staining in another 208 pairs HCC tumor and adjacent non-tumor tissues. (**D** and **E**) Overall survival (**D**) and recurrence free survival (**E**) were evaluated based on IHC staining results of SLC25A35. (**F**) The correlation between SLC25A35 expression and HCC patients' survival were analyzed using the online UALCAN database. (**G-K**) Correlations analysis between the expressions of SLC25A35 and cell proliferation and metastasis markers, including Ki-67 (encoded by the MKI67 gene) (**G**), Snail1 (**H**), Twist1 (**I**), N-cadherin (encoded by the CDH2 gene) (**J**) and Vimentin (encoded by the VIM gene) (**K**) were analyzed in the TCGA HCC data using the online database GEPIA

(Fig. 5E). Consistent with the results from our cohort, prognosis analysis in TCGA cohort using the online UALCAN database also showed that HCC patients with high SLC25A35 expression had significant worse survival than patients with low SLC25A35 expression (Fig. 5F). Moreover, significant positive correlations were existed between the expressions of SLC25A35 and cell proliferation and metastasis markers, including Ki67, Snail1, Twist1, N-cadherin and Vimentin in the TCGA HCC data (Fig. 5G and K), as analyzed by using the online database GEPIA [14]. Together, the above evidence suggests that SLC25A35 may play a crucial role in the malignant progression of HCC.

Further analysis of SLC25A35 expression in pan-cancer using the online database Sangerbox [15] showed that, in line with our observations in HCC, SLC25A35 expression were also significantly upregulated in 10 other types of cancer, including cholangiocarcinoma, the second most common primary liver cancer (Fig S2), providing further evidence for the frequent upregulation of SLC25A35 in human cancers.

SLC25A35 promotes the proliferation and metastasis of HCC cells both in vitro and in vivo

Next, we determined the function of SLC25A35 in HCC. CCK-8 and colony formation assays indicated that knockdown of SLC25A35 suppressed both the short-term and long-term cell proliferation of SNU-739 and SNU-354 cells (Fig. 6A and B). Cell apoptosis and cycle distribution assays using flow cytometry revealed that SLC25A35 knockdown led to significantly increased apoptosis and G1/S cell cycle arrest (Fig. 6C and D). In line with this, EdU staining assay also indicated no significant change in the percentage of proliferating cells upon SLC25A35 knockdown or overexpression (Fig S3A). Using transwell migration and wound healing assays, we found that the migrations of SNU-739 and SNU-354 cells were both markedly suppressed upon SLC25A35 silencing (Fig S3B and 6E). In keeping with this, transwell invasion assay also indicated markedly suppressed invasion abilities of SNU-739 and SNU-354 cells upon SLC25A35 silencing (Fig. 6F). Enhanced epithelial-to-mesenchymal transition (EMT) [16] and increased matrix metalloproteinases (MMPs) production [17] have been considered to play crucial roles in invasiveness of tumor cells. qRT-PCR analysis revealed that SLC25A35 knockdown had no significant effect on expressions of MMPs, including MMP1, MMP2, MMP7 and MMP9, while caused obviously increased expression levels of EMT markers Snail, Twist, N-cadherin and vimentin (Fig S3C and S3D), which is consistent with the results from TCGA data analysis in Fig. 4H and K, suggesting that SLC25A35 may promote HCC metastasis by facilitating EMT.

To validate the above results from in vitro HCC cells, stable SLC25A35 knockdown SNU-739 cells was constructed (Fig S3E and S3F). In the subcutaneous xenograft mice model, the growth rates were lower in SLC25A35 silencing group when compared with control group (Fig. 6G). SLC25A35 silencing group also showed significantly deceased tumor weight as compared with the control group (Fig. 6H). Immunohistochemistry (IHC) staining assay indicated decreased expressions of SLC25A35 in SLC25A35 knockdown group relative to control group (Fig S3G), suggesting that the tumor growth suppressive effect was exerted by SLC25A35 silencing. Hematoxylin and eosin (H&E) staining assay revealed that the number of lung metastases was also reduced when SLC25A35 was knocked-down (Fig. 6I). IHC staining revealed that the expressions of proliferation (Ki-67) and metastasis markers (Snail) were significantly lower in SLC25A35 knockdown group than in control group (Fig S3H and S3I). TUNEL staining assay for cell apoptosis also revealed remarkable decreased percentage of apoptotic cells in SLC25A35 knockdown group, as compared with control group (Fig S3J).

The effects of SLC25A35 overexpression on cell proliferation and metastasis were also evaluated to provide more supports. In CCK-8 and colony formation assays, the proliferation of SNU-368 and HLE cells was significantly enhanced when SLC25A35 was overexpressed (Fig S4A and S4B). In addition, wound healing and transwell migration and invasion assays indicated that the migration and invasion abilities of SNU-368 and HLE cells were all significantly enhanced upon SLC25A35 overexpressing (Fig S4C-S4E).

Additionally, given that SLC25A35 overexpression led to reduced ROS level in HCC cells, the impact of ROS reduction on the proliferation and metastasis were examined in SLC25A35-overexpressing cells. The results showed that restoration of ROS level with H_2O_2 treatment (100 mM for 12 h) did not significantly affect the proliferation and invasion in SLC25A35-overexpressing HCC cells (Fig S5A-S5B), suggesting that ROS reduction does not contribute to the oncogenic functions of SLC25A35 in HCC cells.

Furthermore, to explore the impact of SLC25A35 on the tumor microenvironment in HCC, the correlation between SLC25A35 expression and immune infiltration was analysis using the online Tumor immune estimation resource (TIMER), a web server for comprehensive analysis of tumor-infiltrating immune cells [18]. The results indicate that SLC25A35 expression levels are positively correlated with the infiltration of B cells, CD8 + T cells, CD4 + T cells, macrophages, neutrophils, and dendritic cells in HCC (Fig S6A), suggesting that SLC25A35 may play a role in regulating immune cell infiltration in HCC, which is worthy of further investigation. Additionally, we

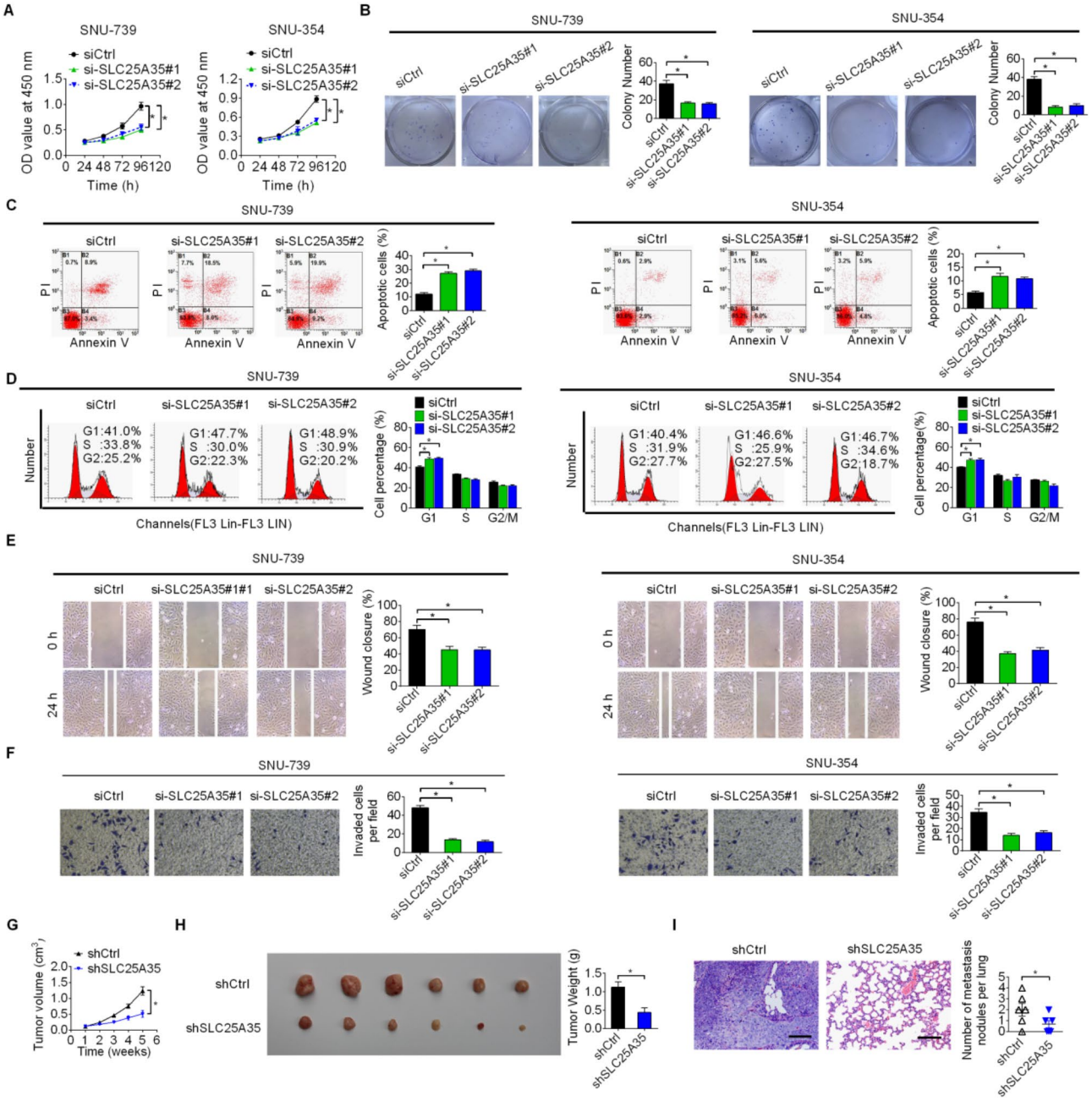

Fig. 6 SLC25A35 promotes the proliferation and metastasis of HCC cells both in vitro and in vivo. (**A** and **B**) CCK-8 (**A**) and colony formation (**B**) assays for short-term and long-term cell proliferation in HCC cells of SNU-739 and SNU-354 with SLC25A35 knockdown. (**C** and **D**) Cell apoptosis (**C**) and cycle distribution (**D**) assays in HCC cells of SNU-739 and SNU-354 with SLC25A35 knockdown. (**E**) Wound healing assay was used to detect the migration abilities of SNU-739 and SNU-354 upon SLC25A35 silencing. (**F**) Matrigel-coated transwell assay was used to determine the invasion abilities of SNU-739 and SNU-354 upon SLC25A35 silencing. (**G**) The growth rate of subcutaneous tumors was compared between SLC25A35 silencing and control groups. (**H**) Gross appearance of tumors from the nude mice and their weights were compared between SLC25A35 silencing and control groups. (**I**) Hematoxylin and eosin (H&E) staining assay was used to compare the number of metastases in the lungs of SLC25A35 silencing and control groups (Scale bars = 50 μm)

evaluated the effect of SLC25A35 on extracellular matrix remodeling. IHC analysis revealed comparable levels of MMP-2 and MMP-9 between the control and SLC25A35 knockdown tumor tissues from nude mice (Fig S6B-S6C), indicating that SLC25A35 may not significantly affect extracellular matrix remodeling.

Forced SLC25A35 expression in liver promotes the carcinogenesis of DEN-induced of HCC

To further explore whether SLC25A35 is a driving factor for hepatocarcinogenesis in vivo, diethylnitrosamine (DEN)-induced HCC mice model was then constructed. The results showed that mice with adeno-associated virus (AAV)-mediated SLC25A35 overexpression had significantly more and larger tumor than the control mice 28 weeks post DEN injection (Fig. 7A), which was further histological verified by H&E staining (Fig. 7B). We also observed higher liver and liver-to-body weight ratio (LW/BW) in SLC25A35 overexpression mice than the control group, which fit the observed phenotypes (Fig. 7C). In line with these findings, higher levels of AST and ALT (molecular marks for liver damage) in serums (Fig. 7D and E) and higher expressions of HCC marks AFP, GPC3, CD44 and Epcam in liver tissues (Fig. 7F) were also

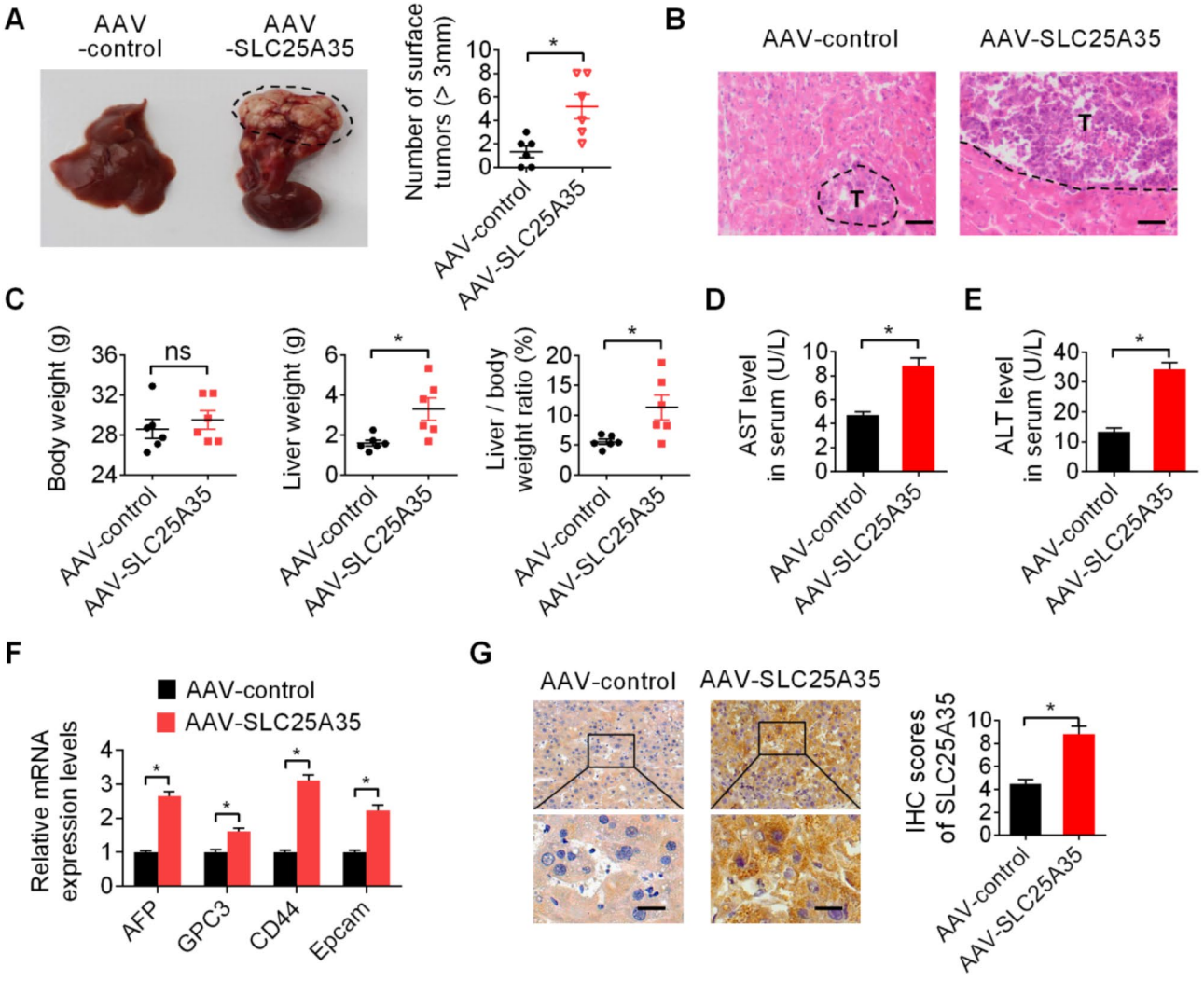

Fig. 7 Forced SLC25A35 expression in liver promotes the carcinogenesis of DEN-induced of HCC. (**A**) Gross appearance of livers from DEN-induced HCC with or without SLC25A35 overexpression and the number of surface tumors were compared. (**B**) Representative H&E staining of livers from DEN-induced HCC mice model with or without SLC25A35 overexpression (Scale bars = 100 μm). (**C**) Liver/body weight ratio of the DEN-induced HCC mice with or without SLC25A35 overexpression. (**D** and **E**) Quantifications of the levels of ALT (**D**) and AST (**E**) in the serums from the DEN-induced HCC mice with or without SLC25A35 overexpression. (**F**) Quantitative RT-PCR analysis for expressions of AFP, GPC3, CD44 and Epcam in the livers from the DEN-induced HCC mice with or without SLC25A35 overexpression. (**G**) IHC staining of SLC25A35 in the livers from DEN-induced HCC mice with or without SLC25A35 overexpression (Scale bars = 20 μm)

observed in SLC25A35 overexpression mice as compared with the control mice. Moreover, the AAV-mediated upregulation of SLC25A35 in the livers of mice were confirmed by IHC staining assay (Fig. 7G), indicating that the oncogenic effect was exerted by forced SLC25A35 expression.

SLC25A35 promotes HCC cell proliferation and invasion by enhancing PGC1α-mediated mitochondrial metabolism

Numerous studies have reported that mitochondrial metabolism plays an important role in the proliferation and metastasis of human cancers [19]. We thus explored whether SLC25A35 promotes the progression of HCC by enhancing PGC1α-mediated mitochondrial metabolism. The results indicated that the suppression of HCC cell proliferation, migration and invasion caused by SLC25A35 silencing could be obviously rescued by PGC-1α overexpression, while the PGC-1α knockdown significantly attenuated the effect of SLC25A35 overexpression on the promotion of HCC cell proliferation, migration and invasion (Fig. 8A and E). These data indicate that SLC25A35 promotes HCC cell proliferation and invasion mainly by enhancing PGC1α-mediated mitochondrial metabolism.

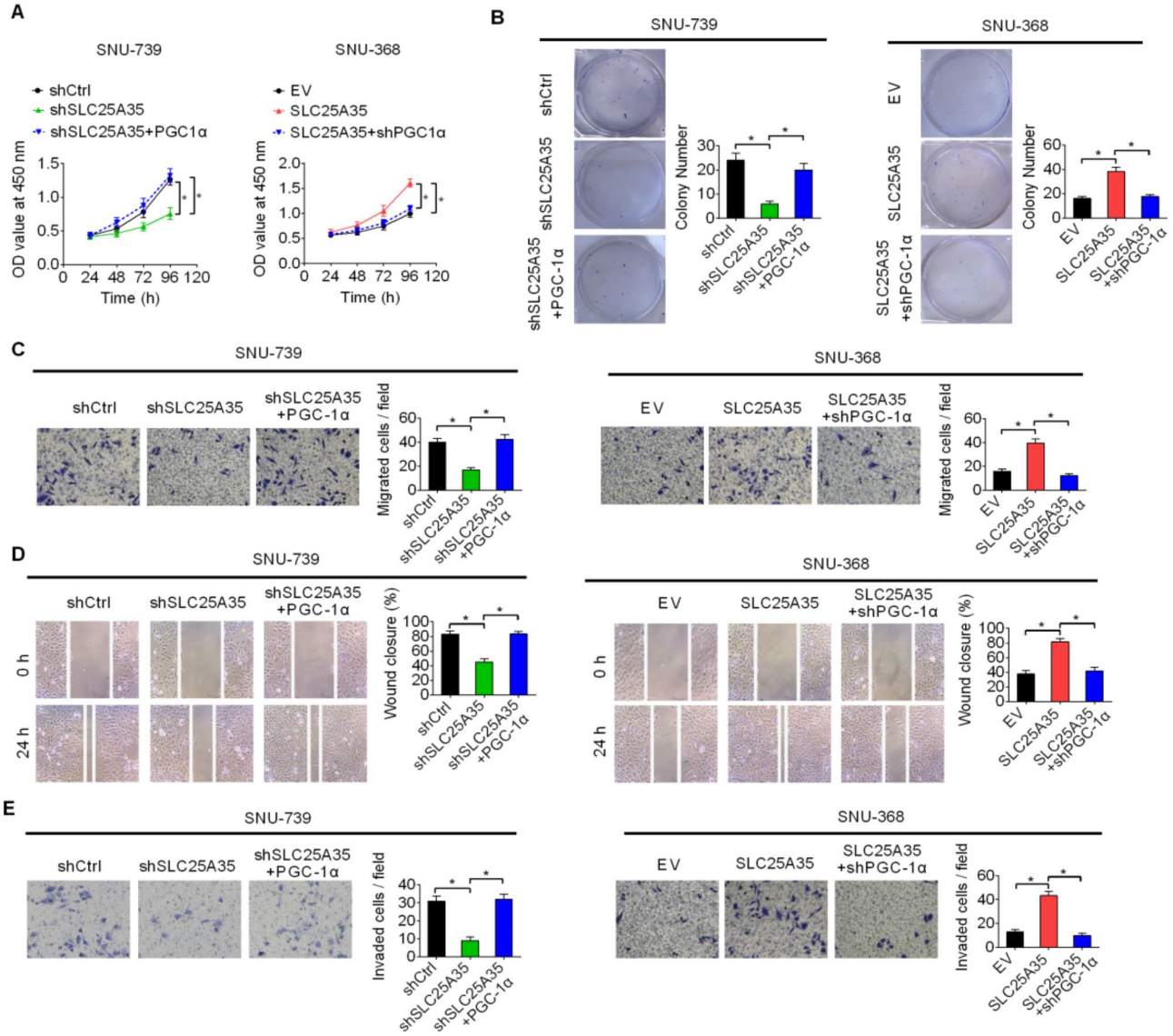

Fig. 8 SLC25A35 promotes HCC cell proliferation and invasion by enhancing PGC1α-mediated mitochondrial metabolism. (**A** and **B**) CCK-8 (**A**) and colony formation (**B**) assays for short-term and long-term cell proliferation in HCC cells with indicated treatment. (**C**-**E**) Transwell migration (**C**), wound healing (**D**) and transwell invasion (**D**) assays were conducted in HCC cells with indicated treatment

SLC25A35 upregulation is caused, at least partially, by decreased miR-663a level in HCC cells

SLC25A35 is upregulated in HCC at both mRNA and protein levels, indicating that SLC25A35 upregulation may occur at transcriptional level. Although a significant negative correlation was found between the mRNA expression and DNA methylation levels of SLC25A35 in HCC by using the online cBioPortal-based [20] bioinformatics analysis (Fig. S7A), the promoter methylation level of SLC125A35 was not changed significantly in HCC (Fig. 9A), implying that SLC44A2 downregulation may not occur at epigenetic level. Given that miRNAs play important roles in tumor progression by regulating expressions of multiple target genes, potential miRNA targeting SLC25A35 was therefore analyzed using the online mirDIP, which is a computational miRNA–target prediction database [21]. Among the top five predicted miRNAs targeting SLC25A35 (Table S7B), transfection with miR-663a significantly reduced SLC25A35 expression, while transfections with other miRNAs showed no obvious effect on SLC25A35 expression (Fig. 9B and C). Bioinformatics analysis using the UALCAN online database [13] and qRT-PCR analysis revealed a significant downregulation of miR-663a in HCC tissues as compared to normal liver tissues (Fig. 9D and Fig S7C). Additionally, significant negative relationships between the expression levels miR-663a and SLC25A35 expressions at both mRNA (n = 30) and protein (n = 208) levels were also existed (Fig. 9E and F). To validate the binding of miR-663a at the 3'-UTR of SLC25A35, a luciferase reporter assay was conducted (Fig. 9G). MiR-663a transfection in HCC cells with wild-type SLC25A35 3'-UTR showed significant decreased luciferase activity, while miR-663a transfection in HCC cells with mutated SLC25A35 3'-UTR showed no significant change in luciferase activity (Fig. 9H). Moreover, miR-663a transfection also attenuated SLC25A35 overexpression-promoted HCC proliferation, migration and invasion (Fig. 9I and L and Fig S7D). Together, these data indicate that SLC25A35 upregulation is caused, at least partially, by decreased miR-663a expression in HCC cells.

Discussion

Cumulative evidences have shown that mitochondrial metabolism plays crucial roles in oncogenesis of various human cancers [22]. However, the mechanisms underlying the activation of mitochondrial metabolism in cancer cells are still not fully understood. SLC25A35 is a member of the SLC25 family that has been speculated as putative antiporter that exchanges dicarboxylates and sulfur oxoanions across mitochondrial inner [9]. However, the role of SLC25A35 in mitochondrial metabolism reprogramming and disease progression remains unexplored in human cancers. Here, we find a crucial oncogenic role for SLC25A35 in the carcinogenesis and progression of HCC by reprogramming PGC-1a-mediated mitochondrial fatty acid oxidation and biogenesis via increasing acetyl-CoA-mediated acetylation of PGC1α. Our findings suggest a crucial oncogenic role of SLC25A35 in HCC by reprogramming mitochondrial metabolism and suggest SLC25A35 as a potential therapeutic target for the treatment of HCC.

The SLC25 mitochondrial carrier family is the largest solute transporter family in mammals with a total of 53 members, which play crucial physiological roles by transporting a variety of compounds across the impermeable mitochondrial inner membrane to linking the cytosol and mitochondrial matrix [8]. Although they were discovered decades ago, their functions in mitochondrial metabolism and physiology remain incompletely understood. SLC25A35 belongs to the SLC25 family of mitochondrial carrier proteins. However, the biological functions of SLC25A35 in mitochondrial remain unexplored [7]. Metabolism reprogramming have been widely accepted as a hallmark of cancer, contributing to tumor cell proliferation, survival and metastasis [23]. Although enhanced aerobic glycolysis has been regarded as the major metabolic change in cancer cells, it is now clear that mitochondrial metabolism also plays crucial roles in oncogenesis [24]. Mitochondria metabolism not only provides building blocks for anabolism of tumor cells, but also necessary to meet the energy demands [25]. Accordingly, mitochondria metabolism has been well recognized as a promising anticancer target [26]. However, the mechanisms underlying the activation of mitochondrial metabolism in tumor cells remains incompletely understood. In the present study, we for the first time demonstrate that SLC25A35 markedly reprogramed mitochondrial metabolism in HCC cells, which was characterized by increased oxygen consumption rate and ATP production and decreased oxidative stress. Subsequent investigation further revealed that enhanced mitochondrial metabolism by SLC25A35 was fueled principally by fatty acid oxidation to not only satisfy the energy demands but also prevent oxidative stress in HCC cells. Meanwhile, SLC25A35 also enhanced mitochondrial biogenesis with no significant effects on the length, length-to-width ratio and expressions of key factors involved in mitochondrial fission and fusion, indicating that SLC25A35 promotes mitochondrial metabolism not by changing their morphology. Together, these data suggest that SLC25A35 plays a critical role in mitochondrial metabolism reprogramming in cancer cells by facilitating FAO and mitochondrial biogenesis. However, the exact substrate of SLC25A35 remains unclear and deserves further exploration.

Peroxisome proliferator–activated receptor gamma coactivator-1 alpha (PGC-1a) is one of the key regulators

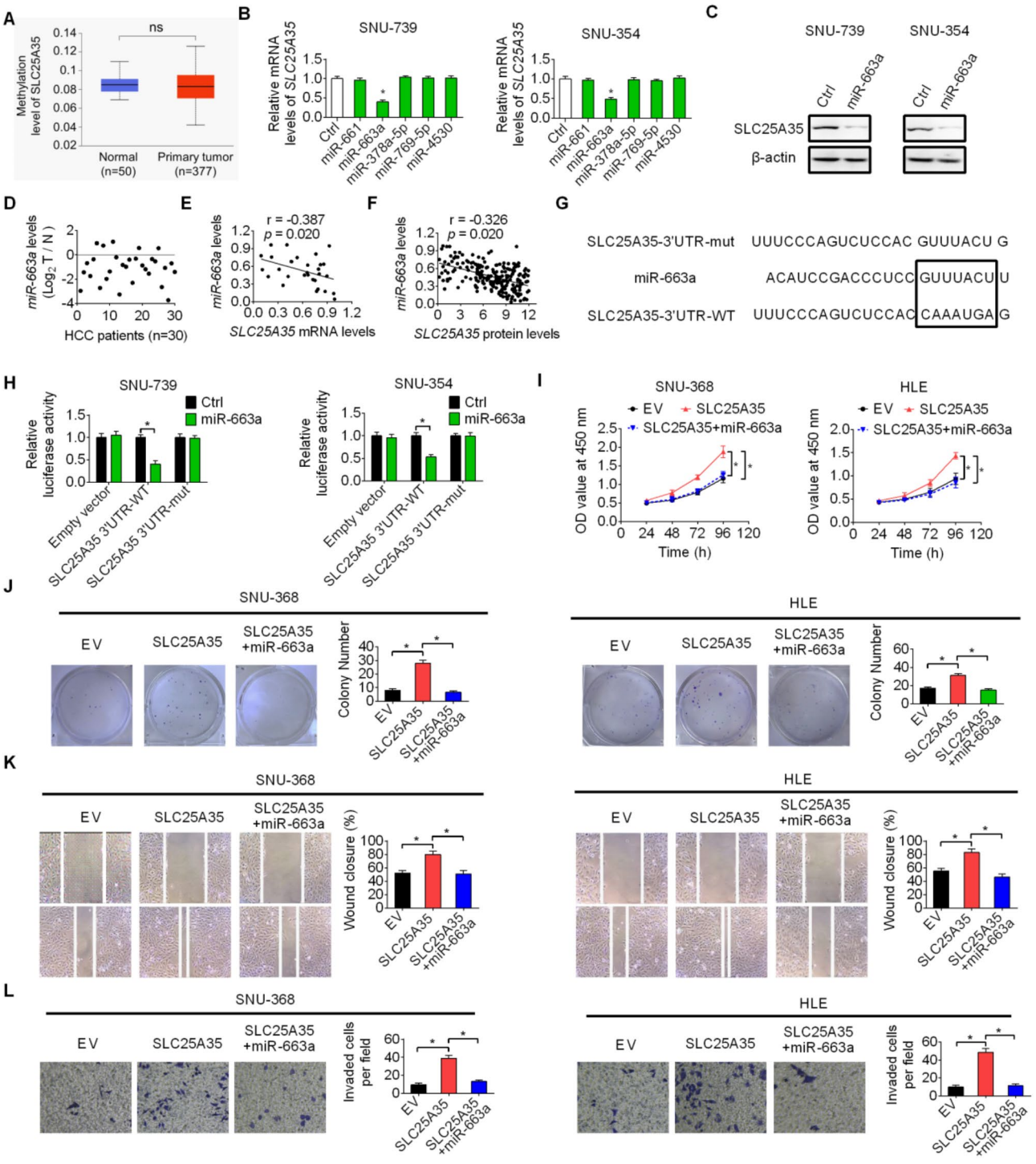

Fig. 9 SLC25A35 upregulation is caused, at least partially, by decreased miR-663a level in HCC cells. (**A**) DNA methylation level of SLC25A35 in HCC was analyzed using the online UALCAN database. (**B** and **C**) SLC25A35 expression was detected by qRT-PCR (**B**) and Western blotting (**C**) analysis in HCC cells transfected with indicated miRNAs. (**D**) The expression levels of miR-663a were analyzed by qRT-PCR assay in HCC (n = 30). (**E** and **F**) Correlations analysis between the expression levels of miR-663a and SLC25A35 expressions at both mRNA (E, n = 30) and protein (F, n = 208) levels were conducted. (**G**) The sequence of wild- or mutant-type of SLC25A35 3′-UTR at the binding sites of miR-663a. (**H**) Luciferase activity was determined in HCC cells with wild- or mutant-type of SLC25A35 3′-UTR upon miR-663a transfection. (**I** and **J**) CCK-8 (**I**) and colony formation (**J**) assays for short-term and long-term cell proliferation in HCC cells with indicated treatment. (**K** and **L**) Wound healing (**K**) and transwell invasion (**L**) assays were conducted in HCC cells with indicated treatment

of mitochondrial biogenesis and oxidation through serving as a transcriptional coactivator with multiple nuclear receptor family transcription factors [12]. It has been well documented that the expression and activity of PGC-1 is tightly regulated by multiple posttranscriptional modifications, such as acetylation, phosphorylation and methylation [11]. However, the molecular factors influencing the acetylation of PGC-1α and thus mitochondrial metabolism in cancer cells remains largely unclear. The present study shows that SLC25A35 downregulates ubiquitin-proteasomal degradation of PGC-1α via increasing acetyl-CoA-mediated acetylation of PGC-1α in HCC cells, further supporting acetylation as a crucial mechanism in the regulation of PGC-1αexpression and activity. Acetyl-CoA not only function as a critical metabolic intermediate in mitochondrial, but also serves as the acetyl group donor for the acetylation of protein [27], supporting the interpretation that fatty acid oxidation and mitochondrial biogenesis are fine-tuned by metabolic state through the change in acetyl-CoA level. Upregulation of PGC-1α by increased acetylation modification could be explained by the competition of acetylation with ubiquitination on the same lysine residue, which still needs more investigations.

Clinically, SLC25A35 was highly expressed in HCC and its upregulation is closely associated with poor prognosis for patients with this malignancy, suggesting SLC25A35 as a potential prognostic marker in HCC. Functional studies showed that SLC25A35 enhanced the proliferation and metastasis of HCC cells both in vitro and in vivo, as well as the carcinogenesis in a DEN-induced HCC mice model. Moreover, the effects of SLC25A35 on the promotion of HCC cell proliferation and invasion could be rescued by PGC-1α, suggesting a crucial oncogenic role for SLC25A35 in the carcinogenesis and progression of HCC by reprogramming PGC-1a-mediated mitochondrial fatty acid oxidation and biogenesis.

Upregulation of SLC25A35 at both mRNA and protein levels suggests a transcriptional regulation mechanism. Even though a negative correlation was existed between the mRNA expression and DNA methylation levels of SLC25A35 in HCC cells, the promoter methylation level of SLC125A35 was comparable between HCC and normal liver tissues, suggesting that the upregulation of SLC25A35 may not occur at epigenetic level. Given that microRNAs (miRNAs) are well-known endogenously expressed small non-coding RNAs that play important role in gene expression and play important roles in tumor progression and and drug resistance by regulating expressions of multiple target genes [28], we therefore explored potential miRNA that contributed to the upregulation of SLC25A35 and found that SLC25A35 is a direct target of miR-663a. Actually, miR-663a has been reported to be downregulated in HCC tissue compared with adjacent non-tumor tissue and inhibits tumor growth, migration and invasion [29, 30]. These findings suggest that SLC25A35 upregulation in HCC is caused, at least partially, by decreased miR-663a level.

In conclusion, our study identified SLC25A35 as a crucial oncogene in HCC by reprogramming mitochondrial metabolism and suggests SLC25A35 as a potential therapeutic target for the treatment of this malignancy.

Limitations of the study: Although our results indicate that SLC25A35 upregulates PGC-1α expression by increasing acetyl-CoA-mediated acetylation of PGC1α, the precise mechanisms through which SLC25A35 elevates cytoplasmic acetyl-CoA are still under investigation. This is partially due to the fact that the specific substrates that SLC25A35 transports within mitochondria are not well-defined. Beside, given that one gene can be targeted by multiple miRNAs, we cannot exclude the possibility that other miRNAs may also contribute SLC25A35 upregulation in HCC.

Supplementary Information

The online version contains supplementary material available at https://doi.org/10.1186/s12964-025-02109-y.

Supplementary Material 1

Author contributions

HY and DW designed the study. HY, LB and LJ contributed to experimental design and study. HY, LB, LJ and YZ performed in vivo and in vitro studies. ZX performed histological analysis. HY and YZ wrote the manuscript. DW reviewed manuscript. All authors reviewed the manuscript.

Funding

This work was supported by National Natural Science Foundation of China (81672341) and Shaanxi Provincial Fund (2019JM-170).

Data availability

No datasets were generated or analysed during the current study.

Declarations

Ethics approval and patient consent

This study was approved by the Ethics Committee of Xijing Hospital of the Air Force Medical University and conducted in line with the instructions of Declaration of Helsinki of the World Medical Association. Written informed consent has been obtained from all participants.

Competing interests

The authors declare no competing interests.

Received: 2 August 2024 / Accepted: 15 February 2025
Published online: 10 March 2025

References

1. McGlynn KA, Petrick JL, El-Serag HB. Epidemiology of Hepatocellular Carcinoma. Hepatology. 2021;73(Suppl 1):4–13.
2. Sugawara Y, Hibi T. Surgical treatment of hepatocellular carcinoma. Biosci Trends. 2021;15:138–41.
3. Martinez-Reyes I, Chandel NS. Cancer metabolism: looking forward. Nat Rev Cancer. 2021;21:669–80.

4. Ma Y, Temkin SM, Hawkridge AM, Guo C, Wang W, Wang XY, Fang X. Fatty acid oxidation: an emerging facet of metabolic transformation in cancer. Cancer Lett. 2018;435:92–100.
5. Anderson RG, Ghiraldeli LP, Pardee TS. Mitochondria in cancer metabolism, an organelle whose time has come? Biochim Biophys Acta Rev Cancer. 2018;1870:96–102.
6. Vasan K, Werner M, Chandel NS. Mitochondrial metabolism as a target for Cancer Therapy. Cell Metab. 2020;32:341–52.
7. Kunji ERS, King MS, Ruprecht JJ, Thangaratnarajah C. The SLC25 Carrier Family: Important Transport Proteins in mitochondrial physiology and Pathology. Physiol (Bethesda). 2020;35:302–27.
8. Ruprecht JJ, Kunji ERS. The SLC25 mitochondrial carrier family: structure and mechanism. Trends Biochem Sci. 2020;45:244–58.
9. Marobbio CM, Giannuzzi G, Paradies E, Pierri CL, Palmieri F. alpha-Isopropylmalate, a leucine biosynthesis intermediate in yeast, is transported by the mitochondrial oxalacetate carrier. J Biol Chem. 2008;283:28445–53.
10. Jeninga EH, Schoonjans K, Auwerx J. Reversible acetylation of PGC-1: connecting energy sensors and effectors to guarantee metabolic flexibility. Oncogene. 2010;29:4617–24.
11. Qian L, Zhu Y, Deng C, Liang Z, Chen J, Chen Y, Wang X, Liu Y, Tian Y, Yang Y. Peroxisome proliferator-activated receptor gamma coactivator-1 (PGC-1) family in physiological and pathophysiological process and diseases. Signal Transduct Target Ther. 2024;9:50.
12. Rius-Perez S, Torres-Cuevas I, Millan I, Ortega AL, Perez S. PGC-1alpha, Inflammation, and Oxidative Stress: An Integrative View in Metabolism. Oxid Med Cell Longev. 2020;2020:1452696.
13. Chandrashekar DS, Karthikeyan SK, Korla PK, Patel H, Shovon AR, Athar M, Netto GJ, Qin ZS, Kumar S, Manne U, et al. UALCAN: an update to the integrated cancer data analysis platform. Neoplasia. 2022;25:18–27.
14. Tang Z, Li C, Kang B, Gao G, Li C, Zhang Z. GEPIA: a web server for cancer and normal gene expression profiling and interactive analyses. Nucleic Acids Res. 2017;45:W98–102.
15. Shen W, Song Z, Zhong X, Huang M, Shen D, Gao P, Qian X, Wang M, He X, Wang T, et al. Sangerbox: a comprehensive, interaction-friendly clinical bioinformatics analysis platform. Imeta. 2022;1:e36.
16. Pastushenko I, Blanpain C. EMT Transition States during Tumor Progression and Metastasis. Trends Cell Biol. 2019;29:212–26.
17. Turunen SP, Tatti-Bugaeva O, Lehti K. Membrane-type matrix metalloproteases as diverse effectors of cancer progression. Biochim Biophys Acta Mol Cell Res. 2017;1864:1974–88.
18. Li T, Fan J, Wang B, Traugh N, Chen Q, Liu JS, Li B, Liu XS. TIMER: a web server for Comprehensive Analysis of Tumor-infiltrating Immune cells. Cancer Res. 2017;77:e108–10.
19. Greene J, Segaran A, Lord S. Targeting OXPHOS and the electron transport chain in cancer; Molecular and therapeutic implications. Semin Cancer Biol. 2022;86:851–9.
20. Gao J, Aksoy BA, Dogrusoz U, Dresdner G, Gross B, Sumer SO, Sun Y, Jacobsen A, Sinha R, Larsson E, et al. Integrative analysis of complex cancer genomics and clinical profiles using the cBioPortal. Sci Signal. 2013;6:pl1.
21. Tokar T, Pastrello C, Rossos AEM, Abovsky M, Hauschild AC, Tsay M, Lu R, Jurisica I. mirDIP 4.1-integrative database of human microRNA target predictions. Nucleic Acids Res. 2018;46:D360–70.
22. Porporato PE, Filigheddu N, Pedro JMB, Kroemer G, Galluzzi L. Mitochondrial metabolism and cancer. Cell Res. 2018;28:265–80.
23. DeBerardinis RJ, Chandel NS. Fundamentals of cancer metabolism. Sci Adv. 2016;2:e1600200.
24. Dave DT, Patel BM. Mitochondrial metabolism in Cancer Cachexia: Novel Drug Target. Curr Drug Metab. 2019;20:1141–53.
25. Oliveira GL, Coelho AR, Marques R, Oliveira PJ. Cancer cell metabolism: rewiring the mitochondrial hub. Biochim Biophys Acta Mol Basis Dis. 2021;1867:166016.
26. Ngoi NYL, Eu JQ, Hirpara J, Wang L, Lim JSJ, Lee SC, Lim YC, Pervaiz S, Goh BC, Wong ALA. Targeting cell metabolism as Cancer Therapy. Antioxid Redox Signal. 2020;32:285–308.
27. Pietrocola F, Galluzzi L, Bravo-San Pedro JM, Madeo F, Kroemer G. Acetyl coenzyme A: a central metabolite and second messenger. Cell Metab. 2015;21:805–21.
28. Rupaimoole R, Slack FJ. MicroRNA therapeutics: towards a new era for the management of cancer and other diseases. Nat Rev Drug Discov. 2017;16:203–22.
29. Huang W, Li J, Guo X, Zhao Y, Yuan X. miR-663a inhibits hepatocellular carcinoma cell proliferation and invasion by targeting HMGA2. Biomed Pharmacother. 2016;81:431–8.
30. Zhang C, Chen B, Jiao A, Li F, Sun N, Zhang G, Zhang J. miR-663a inhibits tumor growth and invasion by regulating TGF-beta1 in hepatocellular carcinoma. BMC Cancer. 2018;18:1179.

Publisher's note